Molecular Imprinting for the Recognition of N-Terminal Histidine Peptides in Aqueous Solution

Bradley R. Hart† and Kenneth J. Shea*

Department of Chemistry, Univerisity of California, Irvine, California 92697-2025

Received January 9, 2002; Revised Manuscript Received May 9, 2002

ABSTRACT: A new procedure for creating macromolecular receptors for peptides using molecular imprinting has been developed. The polymeric receptor exhibits selective uptake of specific N-terminal histidine containing sequences of simple dipeptides. The polymerization and binding are carried out in water. The approach utilizes a strong Ni(II)−His binding to attract the N-terminus histidine of the dipeptide to the polymer surface and secondary interactions between peptide and polymer to discriminate between the peptide sequence. These developments are enabled by utilizing an aqueous based monomer formulation that includes *N*,*N*′-ethylenebis(acrylamide) as a water-soluble cross-linking monomer and a polymerizable NTA ligand, which can be used to incorporate nickel and other metals into these polyacrylamides. The Ni−NTA complex provides a strong histidine binding site that draws the dipeptide to the polymer surface. Mild polymerization conditions that utilize low concentrations of water-soluble initiator and low-temperature result in quantitative polymer yields. Variation of monomer composition reveals an optimum cross-linking for achieving maximum selectivity for these polymers.

Peptide recognition is a theme that governs many essential biological processes. The preparation of artificial receptors capable of recognizing specific amino acid sequences has been a long-standing goal for many researchers working in the area of molecular recognition. Oligopeptides themselves are important targets for recognition[1,2] and also represent an intermediate step toward the recognition of proteins and protein surfaces.[3] Of the many strategies for creating synthetic receptors, molecularly imprinted polymers (MIPs) offer several potential advantages. These include the generality of the approach and the robustness of the recognition element. Amino acids and small peptides have been utilized as templates for molecular imprinting.[4−6] The majority of the reported systems have utilized noncovalent imprinting of protected amino acids and peptides. However, there are some examples of MIPs prepared using metal complexes and covalent imprinting techniques of unprotected amino acids and peptides.[7,8] Here we report the development of molecularly imprinted materials for the sequence selective recognition of short peptides.[9] These materials have been prepared and analyzed in an aqueous environment. In addition, we discuss the kinetics of binding to these materials and the effect of ionic strength on this binding.

Our strategy for creating peptide receptors using molecular imprinting takes advantage of the affinity of N-terminal histidine residues for Ni(II). Preparing a mixed complex between Ni(II), a polymerizable ligand, and an N-terminal histidine peptide provides a template complex, which is then copolymerized with other hydrophilic monomers. Removal of the template peptide leaves behind a region within the polymer that is complementary to the template peptide in size and which contains a Ni(II) complex positioned to bind a N-terminal histidine. By incorporating a Ni(II) complex into the polymer, a handle is provided to bind peptides containing N-terminal histidine residues in water with high affinity.

† Present address: Chemistry and Chemical Engineering Division, Lawrence Livermore National Laboratory, Livermore, CA 94550.

Table 1. Dissociation Constants for Complexation of Histidine with Various Divalent Metal−NTA Complexes

metal	K_d[a,b] (mM)	metal	K_d[a,b] (mM)
Ni^{2+}	0.0093	Co^{2+}	0.114
Cu^{2+}	0.030	Mn^{2+}	3.23
Zn^{2+}	0.112	Pb^{2+}	31.6

[a] All association constants determined by potentiometric titrations. [b] $I = 0.1$ M ($NaClO_4$).

Hochule et al. introduced an adsorbent, based on a Ni(II)−nitrilotriacetic acid (NTA) complex, for protein purification.[10] This ligand occupies four positions in the octahedral coordination sphere of Ni(II), leaving the remaining two for selective interactions. In addition to its use in metal affinity chromatography, the $[Ni(NTA)]^-$ complex has been used in a wide variety of systems for the biofunctionalization of interfaces and for the selective recognition of His-tagged proteins.[11−14]

NTA forms stable 1:1 complexes with Ni(II) with an association constant of over 10^{11}. Histidine has been shown to bind to these complexes at the terminal amine and pyridine nitrogen of the imidazole ring with high affinity (Table 1). In addition, histidine and NTA are known to form 1:1:1 mixed complexes with several divalent metals with varying affinities (Table 1).[15] The orbitals of octahedral (d^8) Ni(II) are hybridized as $sp^3d_{z^2}d_{x^2-y^2}$. This results in two unpaired electrons making these complexes paramagnetic.

The choice of nickel for use in our system over other divalent metals such as copper and zinc was guided by several factors. Nickel provides the highest association constant for the primary interaction, binding of N-terminal histidine residues to $[Ni(NTA)]^-$ (Table 1). In addition, previous reports dealing with the incorporation of Cu(II) complexes into network polyacrylamides have demonstrated poor polymer yields, presumably due to inhibition of in the free radical polymerization by the copper.[16−18] The oxidation of polyacrylamide radicals by Cu(II) in aqueous solution is a facile process.[19−21] This is perhaps due to the low redox potential for the Cu(II)−Cu(I) couple (0.2 V). However, other metals with higher redox potentials, such as Fe(III), are also efficient

10.1021/ma020091f CCC: $22.00
Published on Web 06/26/2002

Scheme 1. Synthesis of NTA−Methacrylamide Ligand 4

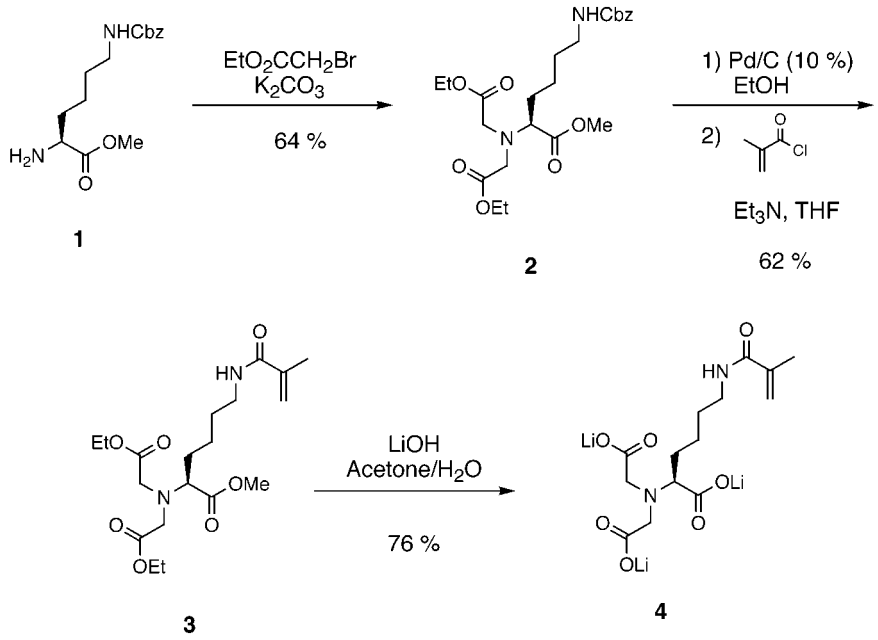

Scheme 2. Synthesis of [Ni(NTA)His]$^{2-}$ Complex 5

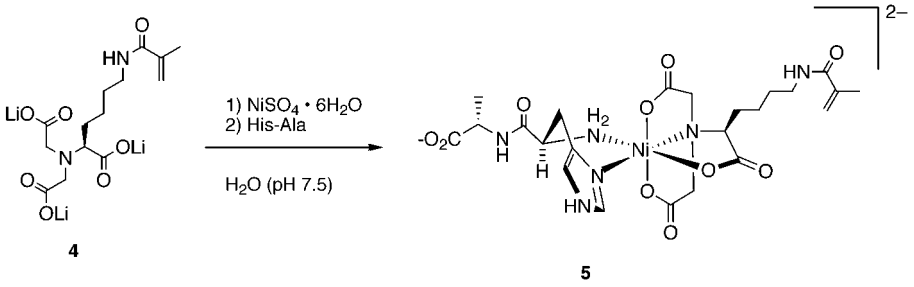

at oxidizing acrylamide radicals.[19] It has been suggested that a simple thermodynamic explanation to describe these processes is inadequate.[19,21]

Covalent incorporation of a polymer bound Ni(NTA) complex to bind N-terminal histidine peptides necessitated the development of a polymerizable form of the NTA lignad. The synthesis of methacrylamide functionalized NTA monomer **4** is shown in Scheme 1. This sequence began with commercially available N^{ϵ}-Cbz-L-lysine methyl ester (**1**). Bis-alkylation of the α-nitrogen of **1** with ethyl bromoacetate in the presence of potassium carbonate provided triester **2**. Deprotection of the ϵ-nitrogen by hydrogenolysis, followed by acylation with methacryloyl chloride, gave amide **3**. Saponification of **3** with lithium hydroxide in acetone/water (3:1) provided triacetate **4**.

The polymerizable mixed complex [Ni(NTA)His-Ala]$^{2-}$ (**5**) was prepared by combining equimolar aqueous solutions of NTA ligand, $NiSO_4 \cdot 6H_2O$, or $Ni(NO_3)_2 \cdot 6H_2O$ and histidine ligand (Scheme 2). The pH of the complex solution was then adjusted to approximately pH 7.5 with 0.1 N NaOH. Confirmation of the octahedral geometry of **5** was made by comparing the electronic spectra for **5** with the known absorbance bands for octahedral complexes of Ni(II).[22] Because of the paramagnetic nature of the metal center, NMR was not useful for characterizing the complex. However, additional evidence for the formation of **5** was obtained by negative-ion electrospray mass spectroscopy. Peaks corresponding to the lithium salt of complex **5** were observed (m/z = 546). In addition, peaks corresponding to [Ni(NTA)]$^-$ were observed (m/z = 385). The relative ratio of **5** to [Ni(NTA)]$^-$ in the mass spectrum was approximately 10:1.4.

There are geometrical constraints placed on the positions of the donor atoms associated with each of the two ligands in **5**, due to the conformations available to these molecules. The two nitrogen donors of histidine must be cis, and the three oxygen donors of the NTA ligand must be meridional. Even with these constraints, there are several isomers which can form. These isomers can be divided into two main groups: those with the imidazole nitrogen of histidine cis to the NTA nitrogen and those with it trans. For each of these two groups, there are three possible orientations of the chiral center-bearing acetate of the NTA ligand with respect to the chiral center on histidine. This equates to a total of six possible diastereomers for complex **5**.

The formation of the mixed complex of Ni(II), polymerizable NTA ligand **4**, and His-Ala was evaluated potentiometrically, and its formation constant was calculated. Similar experiments have been performed with the mixed complex of histidine, NTA, and Ni(II).[23] However, our system differs from that reported in two distinct ways. We have modified the NTA ligand with a polymerizable "tail". In addition, in several instances we have utilized N-terminal histidine peptides as ligands instead of histidine alone. It was not known what effect, if any, these changes would have on complex formation. These studies will permit identification of the

Table 2. Calculated Formation Constant for [Ni(NTA)HisAla]$^{2-}$ and Literature Values for the Formation Constants of [Ni(NTA)His]$^{2-}$ and [Ni(NTA)]$^{-}$

	log K_f
[Ni(NTA)HisAla]$^{2-}$	5.80
[Ni(NTA)His]$^{2-}$	5.03[a]
[Ni(NTA)]$^{-}$	11.5[a]

[a] Literature values from ref 15.

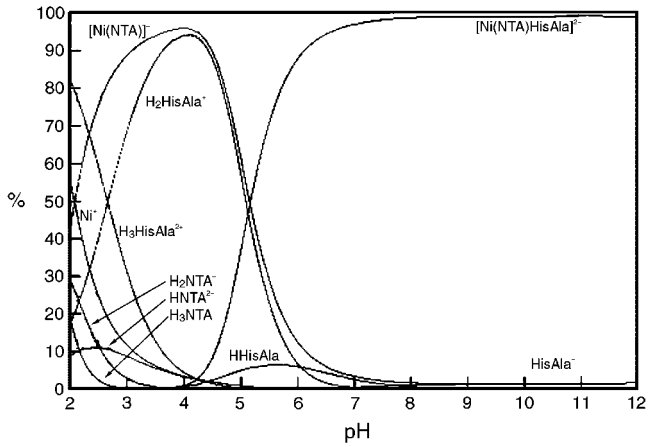

Figure 1. Species distributions of a 0.01 M solution of His-Ala, Ni(II), and NTA ligand **4** for pH values ranging from 2 to 12.

dominant species in solution at various pH values. Additionally, these titrations will be used as a baseline for future potentiometric titrations, which will be performed on polymeric (homogeneous and heterogeneous) systems.

All titrations were carried out using 1.00 N KOH under N_2 in a 10 mL jacketed vessel at 25.0 ± 0.1 °C. The ionic strength of the solution was maintained at 0.1 M with KNO_3. All equilibrium constants were calculated using the computer program Best 7. All details of this type of analysis have been previously described.[24−28] Species distribution curves were obtained from the computer program SPE.[25−28] The log of the formation constant for this 1:1:1 complex was calculated from these data (log K_f = 5.8, Table 2). This compares to the literature value for the association of histidine with [Ni(NTA)]$^{-}$ of log K_f = 5.03.[15]

Figure 1 presents the species distribution diagram for our system with complex component concentrations of 0.01 M. This diagram shows the maximum formation of the 1:1:1 complex at pH > 7.0. There are no other metal-containing species present at this pH. Other species present at lower pH values include [Ni(NTA)]$^{-}$ and diprotonated His-Ala. Both reach a maximum concentration at pH 4.0.

These results indicate that the dipeptide His-Ala has an association constant comparable to histidine for complexation to [Ni(NTA)]$^{-}$. In addition, the modifications we have made to the NTA ligand do not appear to have a detrimental effect on the formation of the 1:1:1 complex.

Polymer Synthesis

In preliminary studies, AIBN (1 mol %) was used as the initiator for the polymerization and required a temperature of at least 65 °C. In addition, a small amount of methanol is required dissolve the AIBN. In an attempt to lower the temperature required for the polymerization and to completely eliminate the use of any cosolvents, a redox initiator system of *N,N′*-tetramethylethylenediamine (TMEDA) and ammonium persulfate (APS) was employed (Scheme 3).[29] This initiator system is water-soluble and is efficient at much reduced temperatures and concentrations when compared to AIBN. In our system, the amount of initiator was reduced from 1 mol % for AIBN to 0.02 and 0.10 mol % for TMEDA and APS, respectively. While persulfate itself is an effective initiator, the rate of polymerization has been shown to increase approximately 3-fold in the presence of TMEDA.[30] Gel times for the polymerization shown in Scheme 3 ranged from approximately 10 to 30 min, depending on the amount of cross-linking monomer used.

In addition to changing the initiator system for these second generation polymers, the total loading of template complex was reduced to 2 mol % (Table 3). By reducing the total amount of Ni^{2+} bound to the polymer, the amount of template required for each polymerization was reduced. This also aids in achieving binding site homogeneity by limiting the possibility of cooperative binding by two metal centers. Table 3 contains the formulations for several polymers prepared with varying amounts of cross-linking monomer.

With the exception of **P-7**, the polymers in Table 3 were all obtained in quantitative yield. HPLC analysis of the postpolymerization extracts of these materials revealed no unreacted monomers or oligimer. In the case of **P-7**, the material never formed a homogeneous gel; rather, the forming polymer precipitated, leaving a significant volume of supernatant solution, which contained large amounts of unreacted monomers. Because of this, polymer **P-7** was omitted from our binding studies. The reactivity ratios for the copolymerization of *N,N′*-ethylenebis(acrylamide) and acrylamide with methacrylamide functionalized complex **5** are not known. However, the reactivity ratios for the copolymerization of acrylamide and methacrylamide have been reported.[31] The calculated polymer composition of our system based on these values indicates a polymer composition very close to the starting monomer composition.

The resulting polymers had textures and physical consistencies that varied depending on the cross-link level. At a low (30%) cross-link level, the polymers were very rubbery when wet. When dried, this polymer became extremely tough and difficult to grind into small particles. At higher cross-linking levels, the materials became less rubbery and were more brittle in the dry state.

The polymers were ground and washed with water (pH = 3−4) to remove the template. Following the acidic wash, the polymer was washed with a solution of 0.02 M $Ni(SO_4)\cdot 6H_2O$ to replace any nickel lost during the acidic wash. The splitting yield was quantified by combining the acid wash fractions and determining the concentration of histidine by HPLC. For polymers **P-1** through **P-6**, template peptide recovery was greater than 90%. The polymer particles were wet sieved, and those particles sized between 38 and 425 μm were used for binding.

Binding isotherms were obtained for N-terminal histidine peptide binding to each polymer at several concentrations. B_{max} was determined by fitting the isotherm data to a one-site binding model. To accurately compare the values of B_{max} for each polymer, it was necessary to normalize the binding data with respect to the nickel content of the polymer. This was necessary

Scheme 3. Synthesis of EBA Cross-Linked Polyacrylamides P-1−P-9 (Pep = Amino Acid Sequence Appended to Histidine)

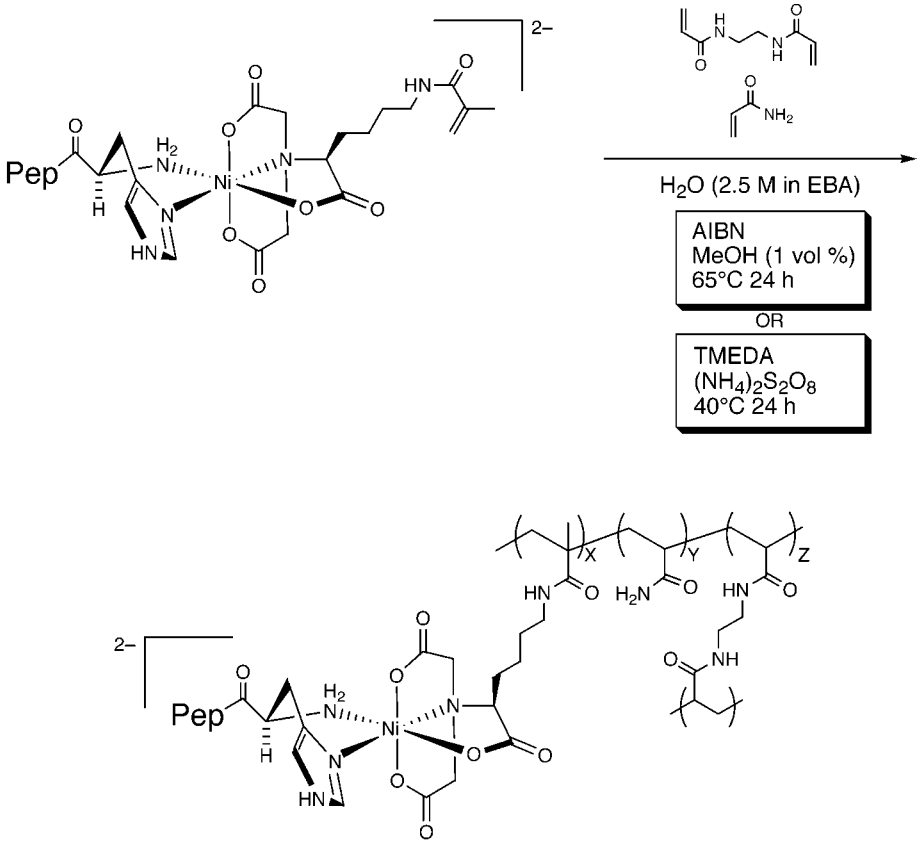

P–1 – P–9

Table 3. Polymerization Formulation Composition for the Synthesis of EBA Cross-Linked Polymer P-1 through P-7

			polymer formulation components (mmol)		
polymer	template peptide	mol % cross-linker	NTA complex	acrylamide	EBA
P-1	His-Ala	80	0.08	0.72	3.20
P-2	His-Ala	70	0.08	1.12	2.80
P-3	His-Ala	60	0.08	1.57	2.35
P-4	His-Ala	50	0.08	1.92	2.00
P-5	His-Ala	40	0.08	2.35	1.57
P-6	His-Ala	30	0.08	2.72	1.20
P-7	His-Ala	10	0.08	3.52	0.40

for two reasons. First, there is some natural variation in nickel content between polymer batches. Second, the polymers are prepared using a mole ratio for the monomers; therefore, the wt % nickel for each of the polymers will not be the same even though the mol % should be similar. The theoretical values of nickel content can be calculated. However, we have found that the nickel content determined by elemental analysis was consistently lower than the theoretical value. Therefore, for each polymer the amount of bound peptide was normalized against the nickel content based on elemental analysis. This normalization manifests itself as the bound concentration (C_b) being expressed as μmol of bound peptide divided by μmol of nickel (μmol bound/μmol Ni). This allows for direct comparison of the peptide uptake observed with these polymers.

Binding isotherms for template His-Ala and His-Phe binding to **P-1**−**P-6** are shown in Figure 2. Values for B_{max} for these peptides as determined from these isotherms are reported in Table 4. The ratio of the His-Ala B_{max} over the His-Phe B_{max} gives some measure of the selectivity of these polymers in terms of capacity. This ratio is termed α and is shown in Table 4 for each of the polymers discussed.

The isotherm for 80% cross-linked **P-1** is shown in Figure 2A. There is clearly an increased capacity for the smaller template peptide His-Ala over His-Phe. The α value for this polymer is 3.3 (Table 4). Figure 2B contains the isotherms for 70% cross-linked **P-2**. There is an obvious increase in capacity for both His-Ala and His-Phe associated with decreasing the cross-linking of the polymer by 10%. However, the selectivity of this polymer is somewhat reduced, giving an α value of 2.2 (Table 4).

A similar situation is observed for 50% cross-linked polymer **P-4** (Figure 2C). There is a large increase in capacity for both peptides with a concomitant reduction in α (Table 4). Interestingly, by decreasing the cross-linking further to 30% in **P-6**, the capacity for both peptides drops to extremely low levels (Figure 2D, Table 4). This also results in a loss of selectivity.

There is an interesting relationship between cross-link density and both selectivity and absolute capacity for these polymers. This dependence is displayed graphically in Figure 3. The capacity, as represented by B_{max} for His-Ala, is maximized at around 50 mol % cross-linker. The decrease in capacity at the higher cross-linking levels is almost certainly due to inaccessibility of some binding sites. The decrease in uptake at lower levels of cross-linking may be due to hydrophobic

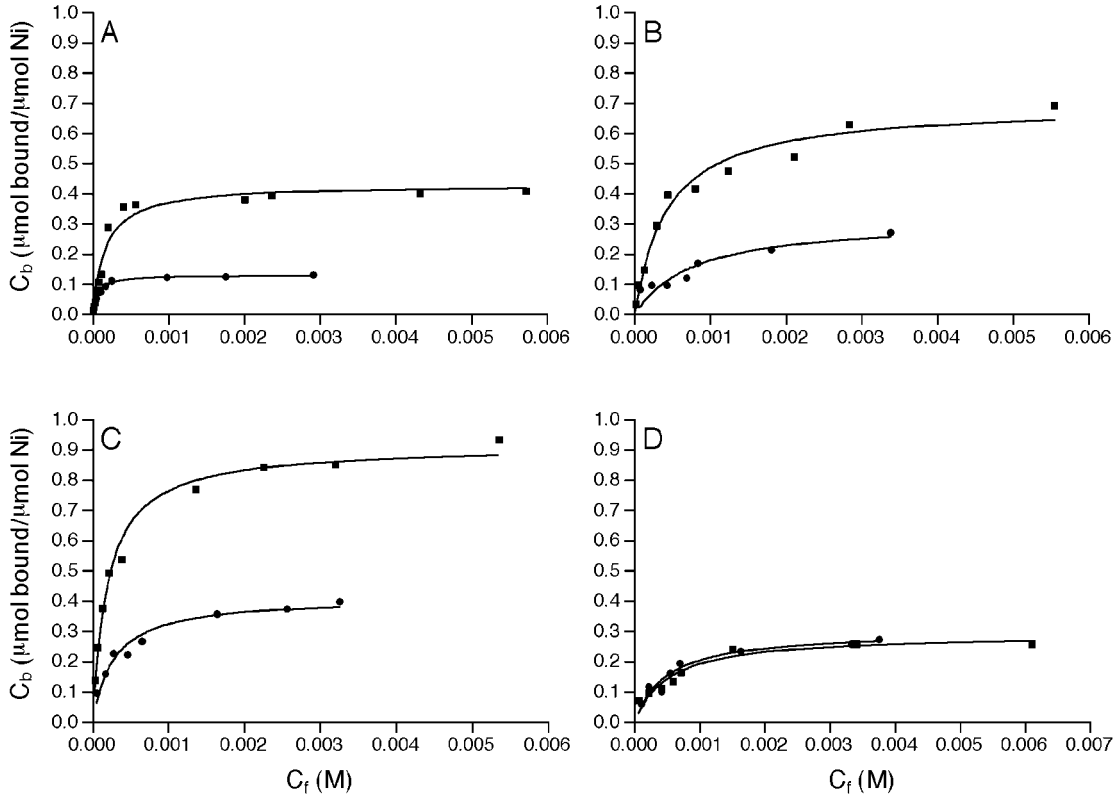

Figure 2. Isotherms showing binding of His-Ala (■) and His-Phe (●) for (A) 80% cross-linked **P-1**, (B) 70% cross-linked **P-2**, (C) 50% cross-linked **P-4**, and (D) 30% cross-linked **P-6**.

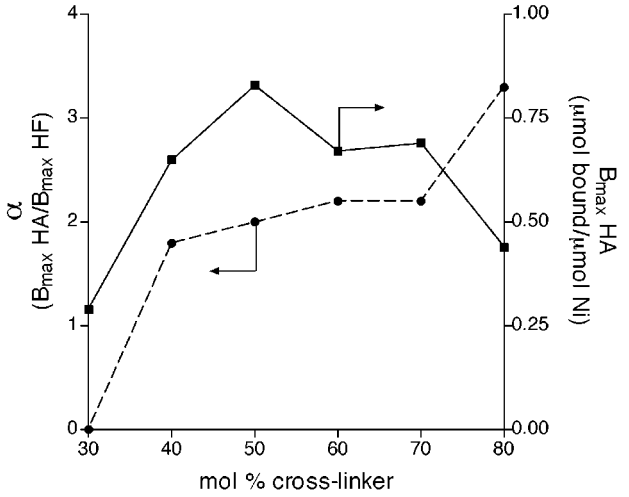

Figure 3. Graph relating the change in α (●, left *Y* axis) and B_{max} HA (■, right *Y* axis) with mol % cross-linker in the polymer.

Table 4. Maximum Binding Capacities for His-Ala and His-Phe Binding, Uptake Selectivity, and Ni(II) Content for P-1 through P-6

polymer	cross-link (mol %)	B_{max} (μmol bound/μmol Ni) His-Ala	B_{max} (μmol bound/μmol Ni) His-Phe	α	Ni content (wt %) measd	Ni content (wt %) theor
P-1	80	0.44	0.13	3.3	0.51	0.76
P-2	70	0.69	0.32	2.2	0.45	0.81
P-3	60	0.67	0.31	2.2	0.42	0.87
P-4	50	0.83	0.41	2.0	0.42	0.93
P-5	40	0.65	0.36	1.8	0.46	1.01
P-6	30	0.29	0.30	1.0	0.48	1.10

collapse of the binding cavities. It seems likely that this phenomenon also results from site inaccessibility within the polymer. The cause of this inaccessibility remains unclear and is currently under investigation.

Figure 3 also indicates that there is a significant dependence of selectivity (α) on cross-link density. The highest α value was obtained with **P-1,** which has the highest cross-link content of all of the polymers studied. This result is understandable, since the observed selectivity appears to result from a size exclusion type model. Although we do not have any information about the pore size distribution of the swollen polyacrylamides, studies indicate that the least amount of swelling is observed for the higher cross-linked polymers. This is likely to result in the observed overall reduction in accessibility with larger analytes being restricted more than smaller ones, thereby resulting in increased selectivity.

The scope of the size selectivity we have observed with His-Ala imprinted polymers was further examined by using His-Phe as the template peptide (**P-8**). The mole fractions of EBA, acrylamide, and template complex were identical to **P-4** and are shown in Table 5. This polymer formulation was chosen on the basis of the results from the cross-link study that indicated 50 mol % cross-linker provided the highest selectivity. This polymer was prepared and processed in exactly the same manner as polymer **P-1** through **P-6**. The splitting yield was found to be 87%.

Table 5. Polymerization Formulation Composition for the Synthesis of EBA Cross-Linked Polymers P-8 and P-9

polymer	template peptide	mol % cross-linker	polymer formulation components (mmol) NTA complex	acrylamide	EBA
P-1	His-Phe	50	0.08	1.92	2.00
P-2	His-$(Ala)_4$	50	0.08	1.92	2.00

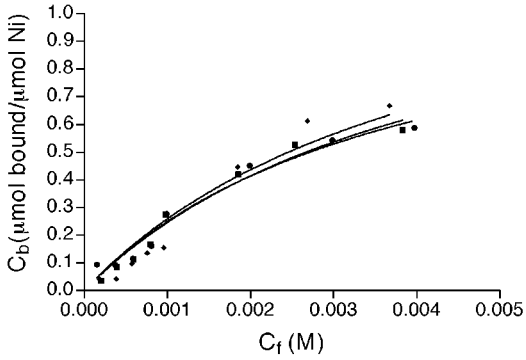

Figure 4. Isotherms showing binding of His-Ala (■), His-Phe (●), and His-Ala-Phe (♦) to **P-8**.

Table 6. Maximum Binding (μmol Bound/μmol Ni) of N-Terminal Histidine Peptides to Polymer P-9

peptide analyte	max binding (μmol bound/μmol Ni)
His-Ala	0.79
His-Phe	0.77
His-Ala-Phe	0.65
His-Ala-Ala-Ala-Ala	0.50
His-Phe-Ala-Ala-Ala	0.49

Batch rebinding analysis of N-terminal histidine peptides His-Phe, His-Ala, and His-Ala-Phe was performed using this polymer. The results were normalized for nickel content as described previously and plotted as C_b (μmol bound/μmol Ni) vs C_f (M) (Figure 4).

We found that the values of B_{max} for His-Ala, His-Phe, and His-Ala-Phe were nearly identical for this polymer (0.7 μmol bound/μmol Ni, Figure 4). This observation fits well with the theory that the size of the template plays a large role in determining the rebinding capacity. The larger phenylalanine residue of the template His-Phe results in the polymer maintaining a high rebinding capacity for peptides with small side chains on the second residue. Interestingly, these data also indicate that steric bulk introduced on the third residue (His-Ala-Phe) does not have an effect on the capacity of the polymer. Perhaps the most important result of this experiment is that it shows that there is no inherent difference in affinity of His-Ala over His-Phe or His-Ala-Phe that might have resulted in the previously observed selectivity.

Extension of this methodology to imprint longer peptide sequences was initiated by imprinting the pentapeptide His-$(Ala)_4$ (**P-9**). This simple peptide was chosen for initial work in order to mirror the work done with the dipeptide His-Ala. It was envisaged that this peptide could be used to analyze the effects of adding steric bulk at positions farther away from the nickel center.

For polymer **P-9**, the mole fractions of EBA, acrylamide, and template complex were identical to **P-4** and **P-8** and are given in Table 4. In addition, this polymer was prepared and processed in the same manner as before. The splitting yield was determined to be 85%.

Batch rebinding analysis of N-terminal histidine peptides His-Phe, His-Ala, and His-Ala-Phe, His-$(Ala)_4$, and His-Phe-Ala-Ala-Ala was performed using this polymer. Single-point binding at high peptide concentrations was performed to obtain the maximum binding for each peptide. The results were normalized for nickel content and are listed in Table 6.

These results show a clear preference for the binding of smaller peptide substrates to **P-9**. The dipeptides His-Ala and His-Phe demonstrate the greatest binding per μmol of nickel.

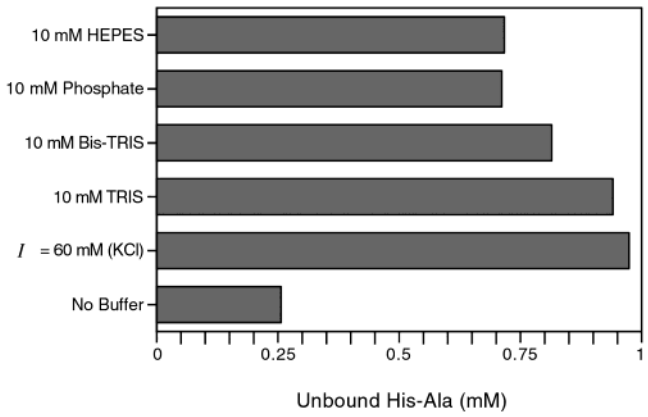

Figure 5. Effect of various buffers and ionic strength on peptide uptake.

In the pentapeptide system, binding capacity seems to be more affected by the length of the peptide sequence. There is practically no difference in uptake of peptides with or without a bulky phenylalanine residue at the second position in the sequence.

The observed results might be expected if the longer peptide template creates, on average, a larger region around the complex that is devoid of polymer chains. The effect might be to reduce the sensitivity of binding to changes in the size of the side chains of the amino acids and, instead, demonstrate selective uptake according to the overall size of the peptide.

Ionic Strength Effects. Initial attempts to perform batch rebinding experiments on these materials using phosphate buffered (30 mM) conditions led to little or no uptake of template dipeptide His-Ala being observed at buffer concentrations as low as 5 mM. To explore this effect, a series of buffers were examined for their effect on binding (Figure 5).

Figure 5 indicates the effect of buffer on binding from the amount of unbound peptide present at equilibrium. These experiments were performed by incubating polymer **P-1** with buffered solutions of 1 mM His-Ala. The amount of unbound peptide was measured at equilibrium and plotted in Figure 5.

All buffers resulted in a decrease in peptide uptake. The smallest effect was observed with 10 mM HEPES and 10 mM phosphate buffers. Interestingly, the largest effect was seen in the absence of buffer, but with the ionic strength of the solution adjusted to 60 mM with KCl. This result indicates that the effect is likely due to changes in the ionic strength of the solution caused by the buffers and not directly related to the buffers themselves. It has been shown that the homogeneous $[Ni(NTA)HA]^-$ complex is not affected by high ionic strength.[15]

One possible explanation is that the polymer structure itself is affected by the presence of dissolved salts. The solution conformation of high molecular weight, charged and uncharged linear polyacrylamides have been reported to be sensitive to disolved salt.[32] These experiments utilized three commercially available polyacrylamides. One of these (Percol 351, $M = 20$ million) was nonionic, another (Percol 721, $M = 20$ million) was polycationic, and another (Percol E-24, $M = 15$ million) was polyanionic. All three of these polymers showed a decrease in the radius of gyration, $\langle r_g \rangle$, when the concentration of NaCl in solution was raised over a

Scheme 4. Solution Phase Synthesis of Dipeptide His-Trp (9)

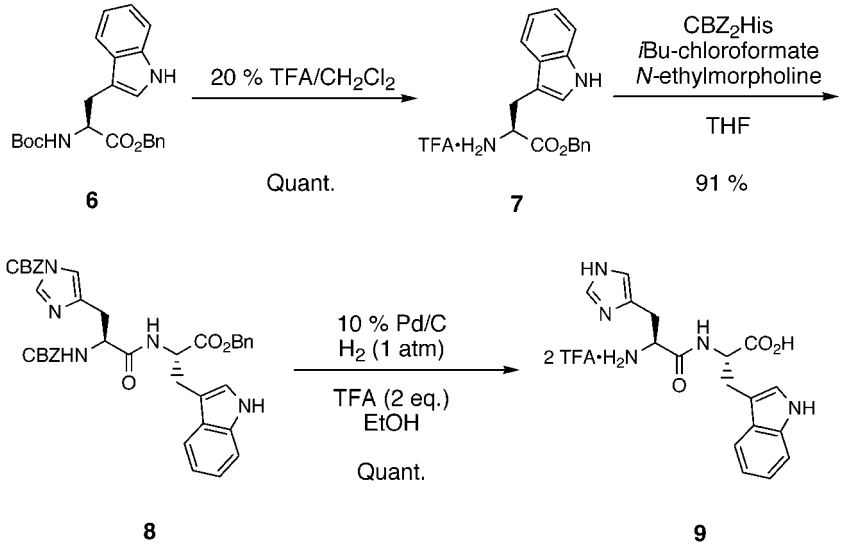

6 **7** **8** **9**

range of 1 mM−1 M. The largest effect was observed between 10 and 100 mM NaCl for the polyanionic polymer where the $\langle r_g \rangle$ was reduced nearly 40. This effect has been attributed to coiling of the polymer chains. Other examples of electrolyte-sensitive polyacrylamides have been observed in highly cross-linked (∼1 mol %)polyanionic polyacrylamide gels.[33] Dissolved salts at concentrations greater than 1 mM brought on a collapse of the gel. These materials were found to shrink to 10−20% of their initial volume.

In the above cases, contraction of the polymer was attributed to shielding of the negative charges within the polymer by the dissolved cations, reducing the effective ionization of the polymer and causing collapse of the polymer chains. Our system is also polyanionic The sources of negative charge from the complex itself, which has an overall −1 charge as the aquo complex and overall −2 when bound to a peptide. In addition, any polymer-bound NTA ligand that is not bound to nickel will have an overall −2 charge at pH 7.5. Despite the fact that network polymers that were used are more highly cross-linked than the materials reported by Tanaka and no visible change in swelling was observed in the presence of dissolved salts, changes in the microenvironment around the binding sites could cause the observed decrease in peptide uptake.

Kinetic Binding Studies. The kinetics of peptide binding to our polymer-bound Ni(II) complexes was explored. In addition to providing information about the time required to reach equilibrium, these experiments provide another way to determine the value of association constants by experimentally measuring the rates of association and dissociation. In these experiments, dipeptide His-Trp (**9**) was used as a fluorescent ligand for the polymer-bound complexes. The synthesis of **9** is shown in Scheme 4. Boc group removal from benzyl ester **6**[34] was achieved by treatment with TFA. Treatment of bis-CBZ-L-histidine with isobutyl chloroformate and *N*-ethylmorpholine, followed by addition of **7**, gave protected dipeptide **8**. Removal of the CBZ and benzyl groups was affected by treatment of **8** with 10% Pd/C and TFA in ethanol under 1 atm of H_2 to give **9**.

Absorbance and fluorescence spectra of **9** were obtained, and it was found to have an absorbance λ_{max} of 278 and a fluorescence λ_{max} of 365. Tryptophan alone has an absorbance λ_{max} of 280 and a fluorescence λ_{max} of 348.[35] A fluorescence calibration curve was prepared for determining the concentration of **9** in solution. Two types of experiments, association and dissociation, were performed to measure k_1 and k_{-1} for the binding of His-Trp to the polymer.

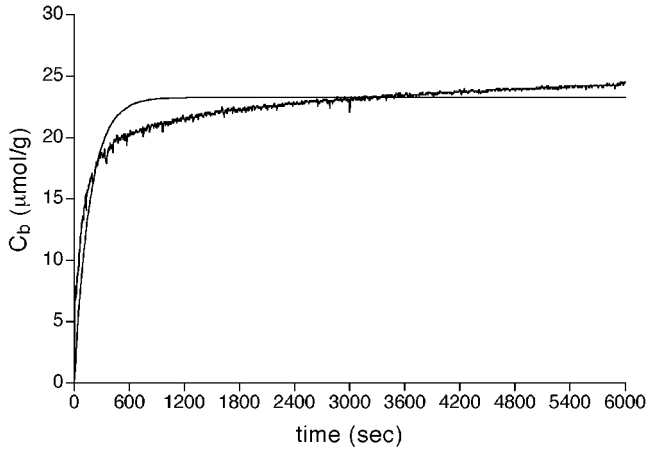

Figure 6. Plot of bound His-Trp (**9**) vs time for association of peptide to polymer **P-4** (jagged line) and best fit line describing the association according to an exponential association expression (smooth line).

Association experiments were performed by adding a solution of **9** (140 μM) to **P-4** (10 mg) and monitoring the fluorescence of the supernatant solution. The concentration of unbound peptide (C_f) in the supernatant was determined by reference to the calibration curve. The concentration of ligand bound to the polymer, C_b, was calculated as described and plotted vs time (Figure 6).

Binding increases over time until it plateaus at Y_{max} at 23 μmol/g. This value represents the amount of binding at equilibrium with this specific concentration of peptide in solution. It is different from B_{max}, which is the amount of binding extrapolated to a very high concentration of ligand. The kinetics of association are defined by a one-phase exponential association. By fitting the data from the association experiment to this equation, we obtained a value for the *observed* rate constant, k_{ob}, of $5.88 \times 10^{-3} \pm 5 \times 10^{-4}$ s^{-1}.

The association data in Figure 6 deviate somewhat from the best fit line—most notably, where the curve

begins to level. This deviation may be due to the fact that we are observing association in a heterogeneous system. After the readily accessible sites within the polymer become saturated, mass transport begins to limit the rate at which molecules are adsorbed by the material. This has the effect of greatly increasing the uncertainty in the value of k_{ob}.

Dissociation experiments were performed by incubating polymer **P-4** with a solution of His-Trp (140 μM) until equilibrium had been reached. The supernatant solution was removed from the polymer followed by addition of water. Release of bound peptide was monitored by fluorescence, and the value of C_b was calculated as before and plotted vs time. Ideally, the concentration of peptide after dilution with fresh solvent should be well below the K_d for the association. However, in this system we are limited by the sensitivity of the fluorescence technique due to the relatively small quantum yield of tryptophan. This requires us to have a fairly high concentration of His-Trp. Because of this, there is competition between association and dissociation so the rate measured is not simply the dissociation rate, but an approach to equilibrium. However, by fitting these data to an exponential decay equation, we are able to obtain an observed rate of dissociation (k_{off}) of $3.21 \times 10^{-4} \pm 4 \times 10^{-6}$ s^{-1}.

The results of these kinetic binding studies indicate that these materials rebind N-terminal histidine peptide substrates with an observed rate constant of $5.88 \times 10^{-3} \pm 5 \times 10^{-4}$ s^{-1}. This allows for equilibration times of under 1 h for these systems. In addition, the high affinity of these peptides for the polymer-bound complexes is reflected in very slow dissociation rates. In the future, it may be possible to perform this experiment using a peptide tagged with a more highly fluorescent probe than simply tryptophan, thus allowing a more accurate determination of k_{off}. It is also important to point out that the data obtained with these experiments pertains to the binding of His-Trp, which may be able to interact with the polymer in ways the previous peptides did not.

Conclusions

We have developed protocols for creating macromolecular receptors for peptides using molecular imprinting. The use of water in the polymer synthesis and recognition steps has obvious advantages over organic systems. Our studies have identified *N,N′*-ethylenebis(acrylamide) as cross-linking monomer that provides good water solubility and can be used to create highly cross-linked polyacrylamides with good stability. We have also developed a polymerizable NTA ligand which can be used to incorporate nickel and other metals into these polyacrylamides. Polymerization conditions have been developed, which allow initiator concentration and temperature to be extremely low while maintaining quantitative polymer yields.

Our results indicate that there is an optimum cross-link density for achieving selectivity in terms of capacity for these polymers. In addition, cross-link density affects the accessibility of the polymer bound nickel sites in a predictable way.

Experimental Section

Instrumentation. All solution NMR spectra were recorded on Bruker Avance DRX spectrometers. Proton spectra were obtained at an operating frequency of 500 MHz. Carbon 13 NMR spectra were obtained at 125.8 MHz. Chromatogrpahic analyte quantification for batch rebinding experiments and splitting yield determination was performed with a Hewlett-Packard 1100 HPLC system equipped with a solvent degassing module, a binary pump module, an autoinjector, a UV/vis variable wavelength detector, and ChemStation software (revision A.06). Calibration curves and tables were prepared and stored in the software with each method. HPLC mobile phases: A = 0.2% (v/v) TFA/H_2O, B = 0.2% (v/v) TFA/CH_3CN.

***N*$^{\epsilon}$-Benzyloxycarbonyl-*N*$^{\alpha}$-bis(2-ethoxy-2-oxoethyl)-L-lysine Methyl Ester (2).** To a solution of *N*-benzyloxycarbonyl-L-lysine methyl ester (1.0 g, 3.4 mmol) in acetonitrile (25 mL) was added ethyl bromoacetate (5.68 g, 34 mmol) followed by finely ground K_2CO_3 (9.4 g, 68 mmol). The reaction mixture was heated at reflux for 18 h. The reaction mixture was filtered through Celite and concentrated. Flash column chromatography of the resulting oil using hexanes to elute the residual ethyl bromoacetate followed by 2:1 hexanes/EtOAc provided triester **2** as a colorless oil (1.300 g, 82%). ^{1}H NMR ($CDCl_3$): δ 7.30 (m, 5 H), 5.08 (s, 2 H), 4.94 (br s, 1 H), 4.11 (q, J = 7.1 Hz, 4 H), 3.7 (s, 3 H), 3.41 (d, J = 17.6 Hz, 2 H), 3.58 (d, J = 17.6 Hz, 2 H), 3.19 (m, 2 H), 1.69 (m, 2 H), 1.52 (m, 2 H), 1.39 (m, 2 H), 1.23 ppm (t, J = 7.1 Hz, 6 H). ^{13}C NMR ($CDCl_3$): δ 173.1, 171.4, 156.4, 136.7, 128.5, 128.1, 128.0, 66.5, 64.5, 60.6, 52.6, 51.4, 40.7, 29.9, 29.3, 22.9, 14.2 ppm. IR (neat): 3380, 2950, 1732, 1526 cm^{-1}. HRMS calcd for $C_{23}H_{35}N_2O_8$ (M + H)$^+$: 467.2393. Found: 467.2401. $[\alpha]^{25}_D = -23.0$ (c = 1.05, ethanol).

***N*$^{\epsilon}$-(2-Methyl-1-oxopropenyl)-*N*$^{\alpha}$-bis(2-ethoxy-2-oxoethyl)-L-lysine Methyl Ester (3).** To a solution of **2** (0.97 g, 1.90 mmol) in ethanol (50 mL) was added 10% Pd/C (10 mg). This solution was stirred vigorously under H_2 (1 atm) for 2 h until no starting material could be seen by TLC (3:2 EtOAc/hexanes). The reaction mixture was filtered through Celite and concentrated in vacuo. The resulting residue was dissolved in THF (50 mL). To this solution was added triethylamine (0.53 mL, 3.8 mmol) followed by dropwise addition of methacryloyl chloride (0.19 mL, 1.9 mmol) in THF (10 mL). The reaction was stirred for 30 min at 0 °C and then for 8 h at 25 °C. The mixture was concentrated. Flash column chromatography of the resulting oil (1:1 EtOAc/hexanes) provided methacrylamide **3** as a colorless oil (0.350 g, 46%). ^{1}H NMR ($CDCl_3$): δ 6.14 (br s, 1 H), 5.67 (s, 1 H), 5.27 (s, 1 H), 5.10 (q, J = 7.1 Hz, 4 H), 3.65 (s, 3 H), 3.61 (d, J = 17.7 Hz, 2 H), 3.57 (d, J = 17.7 Hz, 2 H), 3.40 (t, J = 8.2 Hz, 1 H), 3.27 (m, 2 H), 2.01 (s, 3 H), 1.68 (m, 2 H), 1.60−1.40 (m, 4 H), 1.23 ppm (t, J = 7.1 Hz, 6 H). ^{13}C NMR ($CDCl_3$): δ 173.1, 171.3, 168.5, 140.1, 119.7, 64.3, 60.5, 52.6, 51.4, 39.3, 29.7, 28.6, 23.0, 18.6, 14.1 ppm. IR (neat): 3348, 2935, 1738, 1729 cm^{-1}. HRMS calculated for $C_{19}H_{33}N_2O_7$ (M + H)$^+$: 401.2288. Found: 401.2289. $[\alpha]^{23}_D$ = −27.2 (c = 0.80, ethanol).

***N*$^{\epsilon}$-(2-Methyl-1-oxopropenyl)-*N*$^{\alpha}$-bis(carboxymethyl)-L-lysine Trilithium Salt (4).** To a solution of **3** (2.4 mmol) in 25% H_2O/acetone (30 mL) was added LiOH (7.2 mmol). The reaction was stirred at room temperature for 12 h. Acetone was removed in vacuo, and the resulting aqueous solution was lyophilized to give **4** as a white solid (quantitative yield); mp > 300 °C. ^{1}H NMR (D_2O): δ 5.52 (s, 1 H), 5.29 (s, 1 H), 3.13 (ddd, J = 6.8, 6.8, 2.6 Hz, 2 H), 3.03 (d, J = 17.0 Hz, 2 H), 2.95 (d, J = 17.0 Hz, 2 H), 2.89 (dd, J = 8.6, 5.5 Hz, 1 H), 1.79 (s, 3 H), 1.56 (m, 2 H), 1.43 (m, 2 H), 1.33−1.20 ppm (m, 2 H). ^{13}C NMR (D_2O): δ 181.7, 180.4, 171.3, 138.6, 119.8, 67.3, 56.2, 38.6, 27.7, 27.5, 23.7, 17.0 ppm. IR (KBr): 3396, 2940, 1592, 1413 cm^{-1}.

Trp-OBn·TFA (7). *N*$^{\alpha}$-Boc-L-tryptophan benzyl ester (0.5 g, 1.27 mmol) was dissolved in a solution of 20% TFA in CH_2Cl_2. The reaction mixture was stirred under nitrogen at room temperature for 30 min and evaporated to dryness. Trituration of the resulting oil with Et_2O provided **7** as a white solid (quantitative yield); mp = 143−145 °C. ^{1}H NMR (CD_3CN): δ 9.42 (br s, 1 H), 7.51 (d, J = 8.0 Hz, 1 H), 7.43 (d, J = 8.2 Hz, 1 H), 7.35 (m, 3 H), 7.26 (m, 2 H), 7.16 (m, 2 H), 7.04 (t, J = 7.9 Hz, 1 H), 5.15 (d, J = 12.3 Hz, 1 H), 5.09 (d, J = 12.3 Hz, 1 H), 4.36 (t, J = 6.2 Hz, 1 H), 3.44 ppm (d, J = 6.2 Hz, 2 H).

^{13}C NMR ($CDCl_3$): δ 170.1, 137.6, 136.0, 129.5, 129.4, 129.3, 128.1, 126.2, 122.9, 120.3, 119.1, 112.6, 107.5, 68.8, 54.4, 26.9 ppm. IR (KBr): 3412, 2840, 1742, 1673, 1498, 1205, 1137, 735 cm^{-1}. HRMS calcd for $C_{18}H_{19}N_2O_2$: 294.1368. Found: 294.1362.

CBZ-His(CBZ)-Trp-OBn (8). To a solution of CBZ-L-His-(CBZ)-OH (0.136 g, 0.32 mmol) and *N*-ethylmorpholine (32 μL, 0.25 mmol) in THF (1 mL) and DMF (0.1 mL) at −18 °C was added *i*-butyl chloroformate (42 μL, 0.32 mmol). After an activation period of 10 min, a solution of **7** (0.100 g, 0.25 mmol) and *N*-ethylmorpoholine (42 μL, 0.33 mmol) in THF (1 mL) was added dropwise. The reaction mixture was stirred under nitrogen at −18 °C for 1 h and then overnight at room temperature. The reaction mixture was cooled to 0 °C followed by addition of $NaHCO_3$ (1 mL, 5% aqueous solution). After 10 min this solution was warmed to room temperature and diluted with EtOAc (5 mL). The aqueous layer was removed and washed one time with 5 mL of EtOAc. The organics were combined and washed three times with 10 mL of 1 N HCl, dried over Na_2SO_4, and concentrated. The residue was purified by flash column chromatography (70% EtOAc/haxanes) to provide **8** as a white solid (0.159 g, 91%); mp = 62−64 °C. ^{1}H NMR ($CDCl_3$): δ 8.08 (br s, 1 H), 7.94 (br s, 1 H), 7.43 (m, 6 H), 7.31 (m, 12 H), 7.10 (m, 2 H), 7.01 (m, 1 H), 6.79 (br s, 1 H), 6.45 (br d, J = 6.6 Hz, 1 H), 5.34 (d, J = 12.0 Hz, 1 H), 5.31 (d, J = 12.0 Hz, 1 H), 4.88−5.11 (m, 5 H), 4.60 (br s, 1 H), 3.23 (br m, 2 H), 3.00 (dd, J = 14.8, 5.2 Hz, 1 H), 2.92 ppm (dd, J = 14.8, 5.2 Hz, 1 H). ^{13}C NMR ($CDCl_3$): δ 171.3, 170.6, 156.14, 147.9, 138.3, 136.5, 136.3, 135.9, 135.2, 133.7, 129.2, 128.8, 128.7, 128.6, 128.5, 128.4, 128.3, 128.2, 128.1, 127.3, 123.3, 121.9, 119.4, 118.4, 114.9, 111.1, 109.2, 70.0, 67.0, 66.9, 54.5, 52.6, 29.7, 27.4 ppm. IR (KBr): 3347, 3034, 2927, 1752, 1734, 1670, 1405, 1247, 1012, 742, cm^{-1}. HRMS submitted.

His-Trp·2 TFA (9). To a solution of **8** (0.089 g, 0.127 mmol) and TFA (35 μL) in EtOH (20 mL) under nitrogen was added 10% Pd/C (10 mg). This solution was stirred under H_2 (1 atm) overnight. The reaction mixture was filtered through Celite and evaporated to dryness. Trituration of the resulting oil with Et_2O provided **9** as a white solid in quantitative yield; dec 137−142 °C. ^{1}H NMR (DMSO-d_6): δ 10.64 (s, 1 H), 8.61 (br s, 1 H) 8.06 (s, 1 H), 7.52 (d, J = 7.8 Hz, 1 H), 7.32 (d, J = 7.9 Hz, 1 H), 7.06 (m, 2 H), 6.97 (m, 1 H), 6.87 (s, 1 H), 4.59 (br s, 1 H), 4.08 (dd, J = 7.3, 5.7 Hz, 1 H), 3.20 (dd, J = 14.7, 5.7 Hz, 1 H), 3.04 (dd, J = 14.7, 8.0 Hz, 1 H), 2.95 (dd, J = 15.4, 5.3 Hz, 1 H), 2.82 ppm (dd, J = 15.4, 7.6 Hz, 1 H). ^{13}C NMR (DMSO-d_6): δ 172.7, 167.5, 139.9, 136.1, 137.8, 127.0, 123.8, 121.0, 118.4, 118.1, 116.1, 111.4, 109.3, 53.1, 51.9, 27.7, 27.3 ppm. IR (KBr): 3421, 3144, 3048, 2934, 1676, 1651, 1205, 837, 723 cm^{-1}. HRMS $C_{17}H_{20}N_5O_3$ $(M + H)^+$: 342.1566. Found: 342.1554.

Batch Binding Studies. Stock solutions of the peptide to be analyzed (2.0−7.0 mM) were prepared in distilled, deionized H_2O. Serial dilutions of these solutions provided stock solutions between 0.05 and 7.0 mM. The pH of these solutions was adjusted to pH 7.5 with 0.1 N KOH. 0.50 mL of each stock solution was added to 1 mL HPLC autoinjector vials containing either no polymer or swelled polymer (30 or 60 mg). The vials were shaken overnight at room temperature. The pH of the binding solutions was measured after equilibration to ensure that it did not change. The concentration of unbound analyte, C_f, in the supernatant was determined by HPLC (by reference to a calibration curve) on a C18 (Waters Nova-Pak) 3.9 × 300 mm column. HPLC conditions were 100% mobile phase A for histidine, phenylalanine, and His-Ala and 90:10 A/B for His-Phe, His-Ala-Phe, His-$(Ala)_4$, His-Phe-$(Ala)_3$, and Ala-Phe. After binding, the polymer was washed with MeOH, dried in vacuo, and weighed to determine its dry weight. The concentration of ligand bound to the polymer, C_b, was calculated as described. Data analysis was performed using GraphPad Prism 3.0 software.

Kinetic Association Experiments. To a heterogeneous mixture of **P-4** in 0.5 mL of distilled, deionized H_2O in a fluorescence cuvette was added a solution of His-Trp (**9**, 0.14 μmol) in distilled, deionized H_2O (0.5 mL) with slow stirring. The fluorescence of the supernatant solution was measured once per second at 365 nm with an excitation wavelength of 280 nm. The concentration of unbound peptide (C_f) in the supernatant was determined by reference to the calibration curve. The concentration of ligand bound the polymer, C_b, was calculated as described and plotted vs time.

Kinetic Dissociation Experiments. Dissociation experiments were performed by incubating polymer **P-4** with a solution of His-Trp (0.14 μmol) in distilled, deionized H_2O (1 mL) until equilibrium in a fluorescence cuvette. The supernatant solution was removed from the polymer followed by addition of distilled, deionized H_2O (1 mL). Release of bound peptide was monitored by fluorescence as described for the association experiment.

Polymer Synthesis. To $Ni(SO_4)\cdot 6H_2O$ (0.021 g, 0.08 mmol) in H_2O (0.167 mL) was added peptide template (0.08 mmol) in H_2O (0.100 mL). To this solution was added NTA monomer **4** (0.028 g, 0.08 mmol) in H_2O (0.167 mL). The pH of this solution (pH paper) was adjusted to 7.5−8.0 using 1 N KOH followed by addition of H_2O to bring the total volume to 0.5 mL.

Ethylenebis(acrylamide) (see Table 3 or 5) and acrylamide (see Table 3 or 5) were dissolved in distilled, deionized and O_2-free H_2O (1 mL) with gentle warming in a 1 dram vial. To this solution was added the complex solution described above followed by a solution of TMEDA (0.35 μmol) and ammonium persulfate (1.8 μmol) in H_2O (20 μL). This mixture was purged with nitrogen gas, and then the vial was sealed and heated with an oil bath at 40 °C for 24 h. The resulting blue monolith was ground and washed with water pH 3−4 to remove the template and then washed with H_2O (pH = 7.0, 50 mL). Removal of template was monitored by HPLC, and the splitting yield was calculated by combining the washings and quantifying by HPLC. The particles were sieved to isolate the particles between 38 and 425 μm.

Potentiometric Titrations. All solutions were made with distilled, deionized and carbon dioxide-free water. His-Ala and $Ni(NO_3)_2\cdot 5H_2O$ were purchased from Sigma and Aldrich, respectively. NTA monomer **4** was synthesized as described. The KOH solutions (1.00 N) were standardized against potassium hydrogenophthalate. In all experiments, the ionic strength was maintained at 0.100 with KNO_3 as the supporting electrolyte.

Potentiometric titrations were carried out using 1.00 N KOH (saturated with N_2) with continuous magnetic stirring and under N_2 in a 10 mL jacketed vessel at 25.0 ± 0.1 °C. The vessel was equipped with a gastight cap and fitted with gas inlet and outlet tubes, pH electrode, and manual piston buret. Titrations of His-Ala, 1:1 NTA monomer/Ni(II) and 1:1:1 His-Ala/Ni(II)/NTA monomer were performed. The solution for titration of the 1:1:1 mixed complex was prepared by dissolving 0.10 mmol of each component in 0.1 M KNO_3 solution. The NTA monomer and Ni(II) solutions were combined and transferred to the titration vessel under nitrogen. To this solution was added the His-Ala solution followed by dilution of the mixture to 10 mL. The 1:1 NTA monomer/Ni(II) and His-Ala titration solutions were prepared in a similar manner. All titrations were made after stabilization of the first pH value which was achieved by successive addition of 1.0 M HNO_3 to ensure that the titrations would start from a pH value under 2.5. These solutions were titrated with 1.0 M KOH by addition of 0.02 and 0.01 mL of titrant. The corresponding pH was read and plotted to calculate the values of the overall formation constants of the systems.

All equilibrium constants were calculated using the computer program Best 7. All mathematical details have been previously described.[24−28] Species distribution curves were obtained from the computer program SPE.[25−28]

Acknowledgment. We gratefully acknowledge assistance from Professor Patrick J. Farmer and his research group at UCI, Professor Bruno Szpoganicz at Universidade Federal de Santa Catarina (Brazil) and Dr. Darryl Sasaki at Sandia National Laboratory. Financial support from NIH, NSF and Sandia National Laboratory is gratefully acknowledged. B.H. acknowl-

edges financial support from the University of California in the form of a Regents Dissertation Fellowship.

References and Notes

(1) Hokfelt, T.; Johansson, O.; Ljungdahl, A.; Lundberg, J. M.; Schultzberg, M. *Nature (London)* **1980**, *284*, 515−521.
(2) Hancock, R. E. W. *Lancet* **1997**, *349*, 418−422.
(3) Peczuh, M. W.; Hamilton, A. D. *Chem. Rev.* **2000**, *100*, 2479−2493.
(4) Yu, C.; Mosbach, K. *J. Org. Chem.* **1997**, *62*, 4057−4064.
(5) Kempe, M. *Anal. Chem.* **1996**, *68*, 1948−1953.
(6) Ramstrom, O.; Nicholls, I. A.; Mosbach, K. *Tetrahedron: Asymmetry* **1994**, *5*, 649−656.
(7) Klein, J. U.; Whitcombe, M. J.; Mulholland, F.; Vulfson, E. N. *Angew. Chem., Int. Ed.* . **1999**, *38*, 2057−2060.
(8) Vidyasankar, S.; Ru, M.; Arnold, F. H. *J. Chromatogr.* **1997**, *775*, 51−63.
(9) Hart, B. R.; Shea, K. J. *J. Am. Chem. Soc.* **2001**, *123*, 2072−2073.
(10) Hochuli, E.; Dobeli, H.; Schacher, A. *J. Chromatogr.* **1987**, *411*, 177−184.
(11) Hainfeld, J. F.; Liu, W.; Halsey, C. M. R.; Freimuth, P.; Powell, R. D. *J. Struct. Biol.* **1999**, *127*, 185−198.
(12) Ho, C.; Limberis, L.; Caldwell, K. D.; Stewart, R. J. *Langmuir* **1998**, *14*, 3889−3894.
(13) Dorn, I. T.; Neumaier, K. R.; Tampe, R. *J. Am. Chem. Soc.* **1998**, *120*, 2753−2763.
(14) Sigal, G. B.; Bamdad, C.; Barberis, A.; Strominger, J.; Whitesides, G. M. *Anal. Chem.* **1996**, *68*, 490−497.
(15) Anderegg, G. *Pure Appl. Chem.* **1982**, *54*, 2693−2758.
(16) Sasaki, D. Y. Personal communication.
(17) Dhal, P. K.; Arnold, F. H. *Macromolecules* **1992**, *25*, 7051−7059.
(18) Dhal, P. K.; Arnold, F. H. *New J. Chem.* **1996**, *20*, 695−698.
(19) Collinson, E.; Dainton, F. S.; Smith, D. R.; Trudel, G. J.; Taxuke, S. *Discuss. Faraday Soc.* **1960**, *29*, 188−204.
(20) Collinson, E.; Dainton, F. S.; Mile, B.; Tazuke, S.; Smith, D. R. *Nature (London)* **1963**, *198*, 26−30.
(21) Kochi, J. K. *Science* **1967**, *155*, 415−424.
(22) Greenwood, N. N.; Earnshaw, A. In *Chemistry of the Elements*, 2nd ed.; Butterworth-Heinmann: Oxford, 199; pp 1144−1172.
(23) Israeli, J.; Cecchetti, M. *J. Inorg. Nucl. Chem.* **1968**, *30*, 2709−2716.
(24) Merce, A. L. R.; Szpoganics, B.; Dutra, R. C.; Khan, M. A.; Do Thanh, X.; Bouet, G. *J. Inorg. Biochem.* **1998**, *71*, 87−91.
(25) Schwingel, E. W.; Arend, K.; Zarling, J.; Neves, A.; Szpoganicz, B. *J. Brazil. Chem. Soc.* **1996**, *7*, 31−37.
(26) Martell, A. E.; Motekaitis, R. J. *The Determination and Use of Stability Constants*; 2nd ed.; VCH: New York, 1992.
(27) Li, Y. J.; Martell, A. E. *Inorg. Chim. Acta* **1993**, *214*, 103.
(28) Delgado, R.; Sun, Y.; Motekaitis, R. J.; Martell, A. E. *Inorg. Chem.* **1993**, *32*, 3320−3326.
(29) Feng, X. D.; Guo, X. Q.; Qiu, K. Y. *Makromol. Chem.* **1988**, *189*, 77−83.
(30) Guo, X. Q.; Qiu, K. Y.; Feng, X. D. *Scientia Sinica, B* **1987**, *30*, 897−906.
(31) Kllimchuk, K. A.; Hocking, M. B.; Lowen, S. *J. Polym. Sci., Part A* **2000**, *38*, 3146−3160.
(32) Hocking, M. B.; Klimchuk, K. A.; Lowen, S. *J. Polym. Sci., Part A* **2000**, *38*, 3128−3145.
(33) Tanaka, T. *Sci. Am.* **1981**, *244*, 124−136.
(34) Wang, S.; Gisin, B. F.; Winter, D. P.; Makofske, R.; Kulesha, I. D.; Txougraki, C.; Meienhofer, J. *J. Org. Chem.* **1977**, *42*, 1286−1290.
(35) Creighton, T. E. In *Proteins Structures and Molecular Properties*, 2nd ed.; W. H. Freeman: New York, 1993; p 14.

MA020091F